01 Jan 2006

Novel Sum-of-Sinusoids Simulation Models for Rayleigh and Rician Fading Channels

Chengshan Xiao
Missouri University of Science and Technology, xiaoc@mst.edu

Y. Rosa Zheng
Missouri University of Science and Technology, zhengyr@mst.edu

N. C. Beaulieu

Recommended Citation

C. Xiao et al., "Novel Sum-of-Sinusoids Simulation Models for Rayleigh and Rician Fading Channels," *IEEE Transactions on Wireless Communications*, Institute of Electrical and Electronics Engineers (IEEE), Jan 2006.
The definitive version is available at https://doi.org/10.1109/TWC.2006.256990

Novel Sum-of-Sinusoids Simulation Models for Rayleigh and Rician Fading Channels

Chengshan Xiao, *Senior Member, IEEE,* Yahong Rosa Zheng, *Member, IEEE,* and Norman C. Beaulieu, *Fellow, IEEE*

***Abstract*— The statistical properties of Clarke's fading model with a finite number of sinusoids are analyzed, and an improved reference model is proposed for the simulation of Rayleigh fading channels. A novel statistical simulation model for Rician fading channels is examined. The new Rician fading simulation model employs a *zero-mean* stochastic sinusoid as the specular (line-of-sight) component, in contrast to existing Rician fading simulators that utilize a *non-zero* deterministic specular component. The statistical properties of the proposed Rician fading simulation model are analyzed in detail. It is shown that the probability density function of the Rician fading phase is not only independent of time but also uniformly distributed over $[-\pi, \pi)$. This property is different from that of existing Rician fading simulators. The statistical properties of the new simulators are confirmed by extensive simulation results, showing good agreement with theoretical analysis in all cases. An explicit formula for the level-crossing rate is derived for general Rician fading when the specular component has *non-zero* Doppler frequency.**

***Index Terms*— Fading channel simulator, Rayleigh fading, Rician fading, statistics.**

I. Introduction

MOBILE radio channel simulators are commonly used in the laboratory because they make system tests and evaluations less expensive and more reproducible than field trials. Many different techniques have been proposed for the modeling and simulation of mobile radio channels [1]-[25]. Among them, the well known Jakes' model [3], which is a simplified simulation model of Clarke's model [1], has been widely used for frequency nonselective Rayleigh fading channels for about three decades. Various modifications [9], [16]-[19] and improvements [22], [24], [25] of Jakes' simulator for generating multiple uncorrelated fading waveforms needed for modeling frequency selective fading channels and multiple-input multiple-output (MIMO) channels have been reported. Since Jakes' simulator needs only one fourth the number of low-frequency oscillators as needed in Clarke's model, it is commonly perceived that Jakes' simulator (and its modifications) is more computationally efficient than Clarke's model. However, it was recently established by Pop and Beaulieu [19] that Jakes' simulator and its variants (*e.g.*, [3] and [16]) are not wide sense stationary (WSS) and that "reduction in the number of simulator oscillators based on azimuthal symmetries is meritless". They proposed a Clarke's model-based simulator design having the WSS property in [19], [21]. The Pop-Beaulieu simulator has been employed in a number of diverse applications [26]-[29]. In the first part of this paper, we give a statistical analysis of Clarke's model with a finite number of sinusoids and show that the Pop-Beaulieu simulator has deficiencies in some of its higher-order statistics (as warned in [19, Section III.B]). We then propose an improved version of the Pop-Beaulieu simulator based on Clarke's model for Rayleigh fading channels.

All the existing Rician channel simulation models in the literature assume that the specular (line-of-sight) component is either *constant* and *non-zero* [13], or *time-varying* and *deterministic* [4], [16]. These assumptions may not reflect the physical nature of specular components, particularly when a specular component is random, changing from time to time and from mobile to mobile. Furthermore, according to [4], all these Rician fading models are nonstationary in the wide sense and the probability density function (PDF) of the fading phase is a function of time [4], [16]. In the second part of this paper, a novel statistical simulation model will be proposed for Rician fading channels. The specular component will employ a *zero-mean* stochastic sinusoid with a pre-chosen angle of arrival and a random initial phase. This assumption implies that different specular components in different channels may have different initial phases.

The remainder of this paper is organized as follows. In Section II, we present the statistical properties of Clarke's model with a finite number of sinusoids and show that the Pop-Beaulieu simulator has limitations in its higher-order statistics. An improved simulator for Rayleigh fading channels is proposed. In Section III, we present a novel statistical simulation model for Rician fading channels, and analyze the statistical properties of the new Rician fading model.

Manuscript received February 3, 2005; revised October 6, 2005; accepted November 27, 2005. The editor coordinating the review of this paper and approving it for publication is X. Shen. The work of C. Xiao was supported in part by the National Science Foundation under Grant CCF-0514770 and the University of Missouri-Columbia Research Council under Grant URC-05-064. The work of Y. R. Zheng was supported in part by the University of Missouri System Research Board. The work of N. C. Beaulieu was supported in part by the Alberta Informatics Circle of Research Excellence (*i*CORE). Parts of this paper were previously presented at the IEEE Wireless Communications and Networking Conference (WCNC) 2003, New Orleans, LA, and the IEEE International Conference on Communications (ICC) 2003, Anchorage, AK.

C. Xiao is with the Department of Electrical and Computer Engineering, University of Missouri, Columbia, MO 65211 USA (e-mail: xiaoc@missouri.edu; http://www.missouri.edu/∼xiaoc/).

Y. R. Zheng is with the Department of Electrical and Computer Engineering, University of Missouri, Rolla, MO 65409 USA (e-mail: zhengyr@umr.edu; http://web.umr.edu/∼zhengyr/).

N. C. Beaulieu is with the Department of Electrical and Computer Engineering, University of Alberta, Edmonton, Canada T6G 2G7 (e-mail: beaulieu@ece.ualberta.ca; http://www.ee.ualberta.ca/∼beaulieu/).

Digital Object Identifier 10.1109/TWC.2006.05068

Section IV gives extensive performance evaluations of the new Rayleigh and Rician fading simulators. Section V concludes the paper.

II. An Improved Rayleigh Fading Simulator

Clarke's Rayleigh fading model is sometimes referred to as a mathematical reference model, and is commonly considered as a computationally inefficient model compared to Jakes' Rayleigh fading simulator. In this section, we show that Clarke's model with a finite number of sinusoids can be directly used for Rayleigh fading simulation, and that its computational efficiency and second-order statistics are as good as those of improved Jakes' simulators. We then briefly show that the Pop-Beaulieu simulator has some higher-order statistical deficiencies and improve the model by introducing randomness to the angle of arrival, which leads to improved higher-order statistics.

A. Clarke's Rayleigh Fading Model

The baseband signal of the normalized Clarke's two-dimensional (2-D) isotropic scattering Rayleigh fading model is given by [1], [30]

$$g(t) = \frac{1}{\sqrt{N}} \sum_{n=1}^{N} \exp[j(w_d t \cos \alpha_n + \phi_n)], \tag{1}$$

where N is the number of propagation paths, w_d is the maximum radian Doppler frequency and α_n and ϕ_n are, respectively, the angle of arrival and initial phase of the nth propagation path. Both α_n and ϕ_n are uniformly distributed over $[-\pi, \pi)$ for all n and they are mutually independent.

The central limit theorem justifies that the real part, $g_c(t) = \mathrm{Re}[g(t)]$, and the imaginary part, $g_s(t) = \mathrm{Im}[g(t)]$, of the fading $g(t)$ can be approximated as Gaussian random processes for large N. Some desired second-order statistics for fading simulators are manifested in the autocorrelation and cross-correlation functions which are given in [30] for the case when N approaches infinity. However, the statistical properties of Clarke's model with a finite value of N (number of sinusoids) are not available in the literature. These properties are very important for justifying the suitability of Clarke's model as a valid Rayleigh fading simulator. Thus, we present some of these key statistics here.

Theorem 1: The autocorrelation and cross-correlation functions of the quadrature components, and the autocorrelation functions of the complex envelope and the squared envelope of fading signal $g(t)$ are given by

$$R_{g_c g_c}(\tau) = R_{g_s g_s}(\tau) = \frac{1}{2} J_0(w_d \tau) \tag{2a}$$

$$R_{g_c g_s}(\tau) = R_{g_s g_c}(\tau) = 0 \tag{2b}$$

$$R_{gg}(\tau) = E_{\alpha,\phi}[g^*(t) g(t+\tau)] = J_0(w_d \tau) \tag{2c}$$

$$R_{|g|^2|g|^2}(\tau) = 1 + J_0^2(w_d \tau) - \frac{J_0^2(w_d \tau)}{N}, \tag{2d}$$

where $E_{\alpha,\phi}[\cdot]$ denotes expectation w.r.t. α and ϕ, and $J_0(\cdot)$ is the zero-order Bessel function of the first kind [31].

Proof: The autocorrelation function of the real part of the fading $g(t)$ is proved as follows

$$\begin{aligned} R_{g_c g_c}(\tau) &= E_{\alpha,\phi}\left[g_c(t) g_c(t+\tau)\right] \\ &= \frac{1}{N} \sum_{n=1}^{N} \sum_{i=1}^{N} E_{\alpha,\phi}\left\{\cos(w_d t \cos \alpha_n + \phi_n) \right. \\ &\qquad \left. \cdot \cos[w_d (t+\tau) \cos \alpha_i + \phi_i]\right\} \\ &= \frac{1}{2N} \sum_{n=1}^{N} E_{\alpha}[\cos(w_d \tau \cos \alpha_n)] \\ &= \frac{1}{2N} \sum_{n=1}^{N} \int_{-\pi}^{\pi} \cos\left[w_d \tau \cos \alpha_n\right] \frac{d\alpha_n}{2\pi} \\ &= \frac{1}{2N} \sum_{n=1}^{N} J_0(w_d \tau) = \frac{1}{2} J_0(w_d \tau). \end{aligned}$$

Similarly, one can prove the second part of (2a) and equations (2b)-(2c). The proof of equation (2d) is lengthy and can be treated as a special case of the proof of equation (8d) given in the next subsection. The details are omitted here for brevity. ■

It is noted here that when N approaches infinity, all the derived statistical properties in equations (2) become identical to the desired ones of Clarke's reference model given in [30].

In simulation practice, time-averaging is often used in place of ensemble averaging. For example, the autocorrelation of the real part of the fading signal for one trial (sample of the process) is given by

$$\begin{aligned} \hat{R}_{g_c g_c}(\tau) &= \lim_{T \to \infty} \frac{1}{T} \int_0^T g_c(t) g_c(t+\tau) dt \\ &= \frac{1}{2N} \sum_{n=1}^{N} \cos(w_d \tau \cos \alpha_n). \end{aligned}$$

Clearly, this time averaged autocorrelation changes from trial to trial due to the random angle of arrival. Note that the variance of the time average, $\mathrm{Var}\{\hat{R}_{g_c g_c}(\tau)\} = E\left[|\hat{R}_{g_c g_c}(\tau) - 0.5 J_0(w_d \tau)|^2\right]$, carries important information indicating the closeness between a single trial with finite N and the ideal case with $N = \infty$. We now present the time-averaged variances of the aforementioned correlation statistics.

Theorem 2: The variances of the autocorrelation and cross-correlation of the quadrature components, and the variance of the autocorrelation of the complex envelope of the fading signal $g(t)$ are given by

$$\begin{aligned} \mathrm{Var}\{\hat{R}_{g_c g_c}(\tau)\} &= \mathrm{Var}\{\hat{R}_{g_s g_s}(\tau)\} \\ &= \frac{1 + J_0(2w_d \tau) - 2J_0^2(w_d \tau)}{8N} \end{aligned} \tag{3a}$$

$$\begin{aligned} \mathrm{Var}\{\hat{R}_{g_c g_s}(\tau)\} &= \mathrm{Var}\{\hat{R}_{g_s g_c}(\tau)\} \\ &= \frac{1 - J_0(2w_d \tau)}{8N} \end{aligned} \tag{3b}$$

$$\mathrm{Var}\{\hat{R}_{gg}(\tau)\} = \frac{1 - J_0^2(w_d \tau)}{N}. \tag{3c}$$

Proof: We start with the first equality of eqns. (3a) and (3b) and derive

$$
\begin{aligned}
&\mathrm{Var}\{\hat{R}_{g_cg_c}(\tau)\} \\
&= E\left[\left|\hat{R}_{g_cg_c}(\tau) - \frac{J_0(w_d\tau)}{2}\right|^2\right] \\
&= E\left[\left|\hat{R}_{g_cg_c}(\tau)\right|^2\right] - \frac{J_0^2(w_d\tau)}{4} \\
&= \frac{1}{4N^2}E\left[\sum_{n=1}^{N}\sum_{m=1}^{N}\cos(w_d\tau\cos\alpha_n)\cos(w_d\tau\cos\alpha_m)\right] \\
&\quad -\frac{J_0^2(w_d\tau)}{4} \\
&= -\frac{J_0^2(w_d\tau)}{4} + \frac{1}{4N^2}\left\{\sum_{n=1}^{N}E\left[\cos^2(w_d\tau\cos\alpha_n)\right]\right. \\
&\quad \left.+\sum_{n=1}^{N}\sum_{\substack{m=1\\m\neq n}}^{N}E\left[\cos(w_d\tau\cos\alpha_n)\right]E\left[\cos(w_d\tau\cos\alpha_m)\right]\right\} \\
&= \frac{1}{4N^2}\left[N\cdot\frac{1+J_0(2w_d\tau)}{2} + (N^2-N)J_0^2(w_d\tau)\right] \\
&\quad -\frac{J_0^2(w_d\tau)}{4} \\
&= \frac{1+J_0(2w_d\tau)-2J_0^2(w_d\tau)}{8N}.
\end{aligned}
$$

$$
\begin{aligned}
&\mathrm{Var}\{\hat{R}_{g_cg_s}(\tau)\} \\
&= E\left[\left|\hat{R}_{g_cg_s}(\tau) - 0\right|^2\right] \\
&= \frac{1}{4N^2}E\left[\sum_{n=1}^{N}\sum_{m=1}^{N}\sin(w_d\tau\cos\alpha_n)\sin(w_d\tau\cos\alpha_m)\right] \\
&= \frac{1}{4N^2}\left\{\sum_{n=1}^{N}E\left[\sin^2(w_d\tau\cos\alpha_n)\right]\right. \\
&\quad \left.+\sum_{n=1}^{N}\sum_{\substack{m=1\\m\neq n}}^{N}E\left[\sin(w_d\tau\cos\alpha_n)\right]E\left[\sin(w_d\tau\cos\alpha_m)\right]\right\} \\
&= \frac{1}{4N^2}\left[N\cdot\frac{1-J_0(2w_d\tau)}{2} + 0\right] \\
&= \frac{1-J_0(2w_d\tau)}{8N}.
\end{aligned}
$$

Similarly, we can validate the second equality of eqns. (3a) and (3b). Thus, we have

$$
\begin{aligned}
\mathrm{Var}\{\hat{R}_{gg}(\tau)\} &= E\left[\left|\hat{R}_{gg}(\tau) - J_0(w_d\tau)\right|^2\right] \\
&= E\left[\left|2\hat{R}_{g_cg_c}(\tau) + j2\hat{R}_{g_cg_s}(\tau) - J_0(w_d\tau)\right|^2\right] \\
&= 4E\left[\left|\hat{R}_{g_cg_c}(\tau)\right|^2\right] + 4E\left[\left|\hat{R}_{g_cg_s}(\tau)\right|^2\right] \\
&\quad -J_0^2(w_d\tau) \\
&= \frac{1-J_0^2(w_d\tau)}{N}.
\end{aligned}
$$

This completes the proof of Theorem 2. ■

The results given in Theorems 1 and 2 show that those statistics considered that depend on N, depend on N exclusively as N^{-1}. Therefore, the dependence on N is reduced by increasing N. We shall see later that Clarke's model using a number of sinusoids, $N \geq 8$, can be usefully employed as a Rayleigh fading simulator, in some applications (typically short simulation runs). In applications where the asymptotic variance must be small (typically for long simulation runs), larger values of N (say, 40) can be used for greater simulation accuracy. Its computational efficiency and statistics are similar to those of the recently improved Jakes' models [22], [24], [25], which have removed some statistical deficiencies of Jakes' original model [3] and various modified Jakes' models proposed in [9], [16], [17] and [19].

Before proceeding to further discussion, we make a remark to acknowledge and correct a mistake in [25], which was originally discovered by Sun, Ye and Choi [32]. Specifically, the complex fading process defined by eqn. (14) of [25] may not be a Gaussian random process when the duration of time is very short, and the autocorrelation of the squared envelope of this fading process is nonstationary. However, the problems with this fading process, which arise from a slight over-simplification of earlier results in an associated conference version of the paper, can be easily solved by changing ϕ of (14) in [25] to ϕ_n with ϕ_n being statistically independent and uniformly distributed over $[-\pi, \pi)$ for all n. Actually, in the conference version of [25], the complex fading process was defined correctly; details can be found in (14) of [22]. It is also noted that inspired by Sun *et al* [32], we revisited and corrected the expression for the squared envelope correlation function of the complex fading processes we defined. After the submission of this paper, we also noticed that Patel, Stuber and Pratt [33] have independently discovered the aforementioned mistake in [25].

B. The Pop-Beaulieu Simulator

Based on Clarke's model given by (1), Pop and Beaulieu [19], [21] recently developed a class of wide-sense stationary Rayleigh fading simulators by setting $\alpha_n = \frac{2\pi n}{N}$ in $g(t)$. Thus, the lowpass fading process becomes

$$X(t) = X_c(t) + jX_s(t) \tag{4a}$$

$$X_c(t) = \frac{1}{\sqrt{N}}\sum_{n=1}^{N}\cos\left(w_d t\cos\frac{2\pi n}{N} + \phi_n\right) \tag{4b}$$

$$X_s(t) = \frac{1}{\sqrt{N}}\sum_{n=1}^{N}\sin\left(w_d t\cos\frac{2\pi n}{N} + \phi_n\right). \tag{4c}$$

They warned, however, that while their improved simulator is wide sense stationary (contrary to previous sum-of-sinusoids simulators such as, for example, [3], [16]), it may not model some higher-order statistical properties accurately. Reference [26] reported outstanding agreement between results obtained from one implementation of the Pop-Beaulieu simulator and theory in some turbo decoding applications. However, in general, the quality required of a simulator will depend on the application and some higher-order behaviors may not be accurately modeled using this simulator. To further reveal the

statistical properties of this model, we present the following correlation statistics of this model.

$$R_{X_cX_c}(\tau) = R_{X_sX_s}(\tau) \tag{5a}$$

$$= \frac{1}{2N}\sum_{n=1}^{N}\cos\left(w_d\tau\cos\frac{2\pi n}{N}\right) \tag{5b}$$

$$R_{X_cX_s}(\tau) = -R_{X_sX_c}(\tau) \tag{5c}$$

$$= \frac{1}{2N}\sum_{n=1}^{N}\sin\left(w_d\tau\cos\frac{2\pi n}{N}\right) \tag{5d}$$

$$R_{XX}(\tau) = 2R_{X_cX_c}(\tau) + j2R_{X_cX_s}(\tau) \tag{5e}$$

$$R_{|X|^2|X|^2}(\tau) = 1 + 4R^2_{X_cX_c}(\tau) + 4R^2_{X_cX_s}(\tau) - \frac{1}{N}. \tag{5f}$$

The proof of these statistics shown above is a special case of the proof of Theorem 3 given in the next subsection. The details are omitted here for brevity.

We make three remarks based on (5): 1) These second-order statistics of this modified model with $N = \infty$ are the same as the desired ones of the original Clarke's model. However, when N is finite, the statistics of this model are different from the desired ones derived from Clarke's model; 2) the statistics of this model do not converge asymptotically to the desired ones when N increases as was discussed in [21] for the real part of $R_{XX}(\tau)$; 3) when N is finite and odd, the imaginary part of $R_{XX}(\tau)$, along with $R_{X_cX_s}(\tau)$ and $R_{X_sX_c}(\tau)$, can significantly deviate from zero (the desired value), which implies that the quadrature components of this model are statistically correlated when N is odd.

C. An Improved Rayleigh Fading Channel Simulator

Based on the statistical analyses of Clarke's model and the Pop-Beaulieu simulator, we propose an improved simulation model as follows.

Definition 1: The normalized lowpass fading process of an improved sum-of-sinusoids statistical simulation model is defined by

$$Y(t) = Y_c(t) + jY_s(t) \tag{6a}$$

$$Y_c(t) = \frac{1}{\sqrt{N}}\sum_{n=1}^{N}\cos(w_dt\cos\alpha_n + \phi_n) \tag{6b}$$

$$Y_s(t) = \frac{1}{\sqrt{N}}\sum_{n=1}^{N}\sin(w_dt\cos\alpha_n + \phi_n) \tag{6c}$$

with

$$\alpha_n = \frac{2\pi n + \theta_n}{N}, \qquad n = 1, 2, \cdots, N \tag{7}$$

where ϕ_n and θ_n are statistically independent and uniformly distributed over $[-\pi, \pi)$ for all n. It is noted that the difference between this improved model and the Pop-Beaulieu simulator is the introduction of random variables θ_n to the angle of arrival. Randomizing θ_n slightly decreases the efficiency of the simulator, but significantly improves the statistical quality of the simulator. This model differs from Clarke's model in that it forces the angle of arrival, α_n, to have a value restricted to the interval $\left[\frac{2n\pi-\pi}{N}, \frac{2n\pi+\pi}{N}\right)$. The angle of arrival is random and uniformly distributed inside this sector, in contrast to being fixed as it is in Jakes' model and in the Pop-Beaulieu simulator. Clarke's model and a simulator proposed by Hoeher [7], assume independent α_n, each uniformly distributed on $[-\pi, \pi)$. Although our simulator design requires generating the same number of random α_n, it ensures a more uniform empirical distribution of α_n, particularly for small values of N, (but does not fix the values of α_n). We shall see subsequently that this modification reduces the variances of the empirical simulator statistics. It can be shown that the first-order statistics of this improved model are the same as those of the Pop-Beaulieu simulator. However, some second-order statistics of this improved model are different, and they are presented below.

Theorem 3: The autocorrelation and cross-correlation functions of the quadrature components, and the autocorrelation functions of the complex envelope and the squared envelope of fading signal $Y(t)$ are given by

$$R_{Y_cY_c}(\tau) = R_{Y_sY_s}(\tau) = \frac{1}{2}J_0(w_d\tau) \tag{8a}$$

$$R_{Y_cY_s}(\tau) = R_{Y_sY_c}(\tau) = 0 \tag{8b}$$

$$R_{YY}(\tau) = J_0(w_d\tau) \tag{8c}$$

$$R_{|Y|^2|Y|^2}(\tau) = 1 + J_0^2(w_d\tau) - f_c(w_d\tau, N) - f_s(w_d\tau, N), \tag{8d}$$

where

$$f_c(w_d\tau, N) = \sum_{k=1}^{N}\left[\frac{1}{2\pi}\int_{\frac{2\pi k-\pi}{N}}^{\frac{2\pi k+\pi}{N}}\cos(w_d\tau\cos\gamma)d\gamma\right]^2 \tag{9a}$$

$$f_s(w_d\tau, N) = \sum_{k=1}^{N}\left[\frac{1}{2\pi}\int_{\frac{2\pi k-\pi}{N}}^{\frac{2\pi k+\pi}{N}}\sin(w_d\tau\cos\gamma)d\gamma\right]^2. \tag{9b}$$

The proof of this theorem is lengthy; a proof is outlined in Appendix I.

We now present the time-averaged variances of some key correlation statistics of $Y(t)$ in Theorem 4.

Theorem 4: The variances of the autocorrelation and cross-correlation of the quadrature components, and the variance of the autocorrelation of the complex envelope of the fading signal $Y(t)$ are given by

$$\mathrm{Var}\{\hat{R}_{Y_cY_c}(\tau)\} = \mathrm{Var}\{\hat{R}_{Y_sY_s}(\tau)\} = \frac{1 + J_0(2w_d\tau)}{8N} - \frac{f_c(w_d\tau, N)}{4} \tag{10a}$$

$$\mathrm{Var}\{\hat{R}_{Y_cY_s}(\tau)\} = \mathrm{Var}\{\hat{R}_{Y_sY_c}(\tau)\} = \frac{1 - J_0(2w_d\tau)}{8N} - \frac{f_s(w_d\tau, N)}{4} \tag{10b}$$

$$\mathrm{Var}\{\hat{R}_{YY}(\tau)\} = \frac{1}{N} - f_c(w_d\tau, N) - f_s(w_d\tau, N). \tag{10c}$$

Proof: The proof of this theorem is similar to that of Theorem 2; details are omitted for brevity. ∎

As can be seen from Theorems 1 and 3, the correlation statistics, except the autocorrelation of the squared envelope, of the improved model are the same as those of Clarke's model when both models have the same number of sinusoids. Fig. 1 shows that the autocorrelations of the squared envelope for Clarke's model (2d) and for the new model (8d) are similar, and that this statistic for $N = 8$ is closer to the ideal

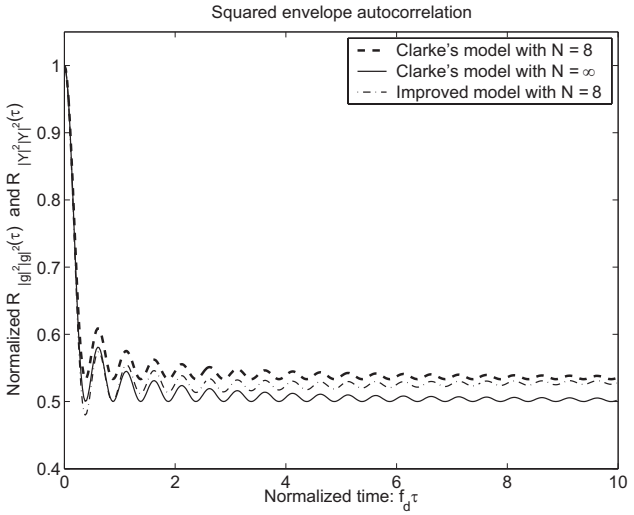

Fig. 1. Theoretical autocorrelations of the squared envelopes of Clarke's model and our improved model.

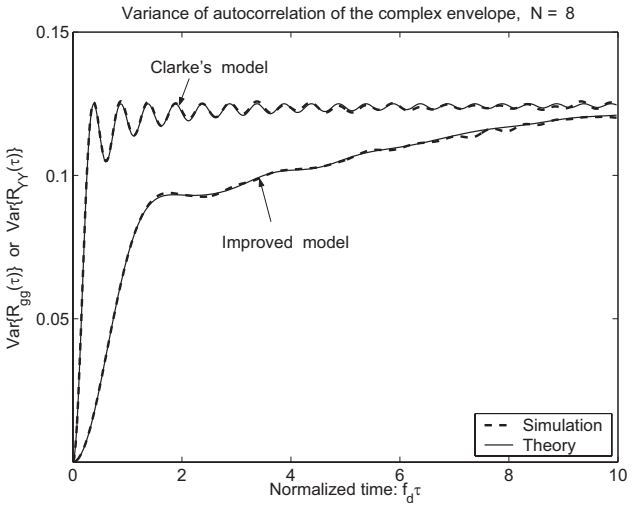

Fig. 2. Variances of autocorrelations of the complex envelope of Clarke's model and our improved model.

value ($N = \infty$) for the improved simulator than for Clarke's model. However, the *variances* of the empirical correlations of the improved model are smaller than the empirical correlation variances of Clarke's model. Using Theorems 2 and 4, Fig. 2 shows, as an example, some theoretical results and the corresponding simulation results for the correlation variances of Clarke's model and the improved model. Obviously, the variances of the autocorrelation of the complex envelope of our improved model are smaller than those of Clarke's model. This implies that the improved simulator converges faster than Clarke's model (and Hoeher's simulator) to an average value for a finite number of simulation trials.

III. A Novel Rician Fading Simulator

In this section, we present a statistical Rician fading simulation model and its statistical properties.

Definition 2: The normalized lowpass fading process of a new statistical simulation model for Rician fading is defined by

$$Z(t) = Z_c(t) + jZ_s(t) \tag{11a}$$

$$Z_c(t) = \left[Y_c(t) + \sqrt{K}\cos(w_d t\cos\theta_0 + \phi_0)\right]/\sqrt{1+K} \tag{11b}$$

$$Z_s(t) = \left[Y_s(t) + \sqrt{K}\sin(w_d t\cos\theta_0 + \phi_0)\right]/\sqrt{1+K} \tag{11c}$$

where K is the ratio of the specular power to scattered power, θ_0 and ϕ_0 are the angle of arrival and the initial phase, respectively, of the specular component, and ϕ_0 is a random variable uniformly distributed over $[-\pi, \pi)$.

A Rician fading simulator having a specular component with a non-zero Doppler frequency was studied in [16]. Our simulator model (11) is different from the simulator in [16] because in our model the initial phase of the specular component is considered a random variable uniformly distributed over $[-\pi, \pi)$, while the initial phase of the specular component in [16] is assumed to be constant. This is an important difference since it results in a wide-sense stationary model for our case, whereas the model in [16] is nonstationary.

We present the ensemble correlation statistics of the fading signal, $Z(t)$, in the following theorem.

Theorem 5: The autocorrelation and cross-correlation functions of the quadrature components, and the autocorrelation functions of the complex envelope and the squared envelope of fading signal $Z(t)$ are given by

$$\begin{aligned} R_{Z_cZ_c}(\tau) &= R_{Z_sZ_s}(\tau) \\ &= \left[J_0(w_d\tau) + K\cos(w_d\tau\cos\theta_0)\right]/(2+2K) \end{aligned} \tag{12a}$$

$$\begin{aligned} R_{Z_cZ_s}(\tau) &= -R_{Z_sZ_c}(\tau) \\ &= K\sin(w_d\tau\cos\theta_0)/(2+2K) \end{aligned} \tag{12b}$$

$$\begin{aligned} R_{ZZ}(\tau) = [&J_0(w_d\tau) + K\cos(w_d\tau\cos\theta_0) \\ &+ jK\sin(w_d\tau\cos\theta_0)]/(1+K) \end{aligned} \tag{12c}$$

$$\begin{aligned} R_{|Z|^2|Z|^2}(\tau) = \{&1 + J_0^2(w_d\tau) + K^2 - f_c(w_d\tau, N) - f_s(w_d\tau, N) \\ &+ 2K\left[1 + J_0(w_d\tau)\cos(w_d\tau\cos\theta_0)\right]\}/(1+K)^2. \end{aligned} \tag{12d}$$

The proof of Theorem 5 is given in Appendix II.

Based on Definition 2 and Theorems 4 and 5, we present the following corollary omitting the proof.

Corollary: The variances of the autocorrelation and cross-correlation of the quadrature components, and the variance of the autocorrelation of the complex envelope of the fading signal $Z(t)$ are given by

$$\begin{aligned} \mathrm{Var}\{\hat{R}_{Z_cZ_c}(\tau)\} &= \mathrm{Var}\{\hat{R}_{Z_sZ_s}(\tau)\} \\ &= \left[\frac{1+J_0(2w_d\tau)}{8N} - \frac{f_c(w_d\tau, N)}{4}\right]/(1+K)^2 \end{aligned} \tag{13a}$$

$$\begin{aligned} \mathrm{Var}\{\hat{R}_{Z_cZ_s}(\tau)\} &= \mathrm{Var}\{\hat{R}_{Z_sZ_c}(\tau)\} \\ &= \left[\frac{1-J_0(2w_d\tau)}{8N} - \frac{f_s(w_d\tau, N)}{4}\right]/(1+K)^2 \end{aligned} \tag{13b}$$

$$\mathrm{Var}\{\hat{R}_{ZZ}(\tau)\} = \frac{[1/N - f_c(w_d\tau, N) - f_s(w_d\tau, N)]}{(1+K)^2} \tag{13c}$$

where $f_c(w_d\tau, N)$ and $f_s(w_d\tau, N)$ are given by (9). Note that when the number of sinusoids, N, is fixed, the variances of the aforementioned correlation statistics tends to be smaller as the Rice factor, K, increases.

We now present the PDF's of the fading envelope $|Z(t)|$ and phase $\Psi(t) = \arctan[Z_c(t), Z_s(t)]$[1].

Theorem 6: When N approaches infinity, the envelope $|Z(t)|$ is Rician distributed and the phase $\Psi(t)$ is uniformly distributed over $[-\pi, \pi)$, and their PDF's are given by

$$f_{|Z|}(z) = 2(1+K)z \cdot \exp\left[-K-(1+K)z^2\right] \cdot I_0\left[2z\sqrt{K(1+K)}\right], \quad z \geq 0 \tag{14a}$$

$$f_{\Psi}(\psi) = \frac{1}{2\pi}, \quad \psi \in [-\pi, \pi) \tag{14b}$$

respectively, where $I_0(\cdot)$ is the zero-order modified Bessel function of the first kind [31].

Proof: Since the random sinusoids in the sums of $Y_c(t)$ and $Y_s(t)$ are statistically independent and identically distributed, $Y_c(t)$ and $Y_s(t)$ tend to Gaussian random processes as the number of sinusoids, N, increases without limit, according to a central limit theorem [34]. Moreover, since $R_{Y_cY_s}(\tau) = 0$ and $R_{Y_sY_c}(\tau) = 0$, $Y_c(t)$ and $Y_s(t)$ are uncorrelated and asymptotically independent. Let $m_c(t) = \sqrt{\frac{K}{1+K}}\cos(w_d t\cos\theta_0 + \phi_0)$ and $m_s(t) = \sqrt{\frac{K}{1+K}}\sin(w_d t\cos\theta_0 + \phi_0)$. Then, $[Z_c(t) - m_c(t)]$ and $[Z_s(t) - m_s(t)]$ are uncorrelated and asymptotically independent.

Given an initial phase ϕ_0 of the specular component, the conditional joint PDF of $Z_c(t)$ and $Z_s(t)$ can be derived as follows

$$\begin{aligned} &f_{Z_c,Z_s}(z_c, z_s|\phi_0) \\ &= \frac{1+K}{\pi}\exp\left\{-(1+K)\left[z_c - m_c\right]^2 - (1+K)\left[z_s - m_s\right]^2\right\} \\ &= \frac{1+K}{\pi}\exp\left\{-(1+K)(z_c^2+z_s^2) - K \right. \\ &\qquad \left. +2(1+K)[z_c m_c + z_s m_s]\right\}. \end{aligned}$$

Since the initial phase ϕ_0 is uniformly distributed over $[-\pi, \pi)$, the joint PDF of $Z_c(t)$ and $Z_s(t)$ is given by

$$\begin{aligned} f_{Z_c,Z_s}(z_c, z_s) &= \int_{-\pi}^{\pi} f_{Z_c,Z_s}(z_c, z_s|\phi_0)\cdot\frac{1}{2\pi}\cdot d\phi_0 \\ &= \frac{1+K}{\pi}\exp\left[-(1+K)(z_c^2+z_s^2) - K\right] \\ &\quad \cdot \int_{-\pi}^{\pi}\exp\left\{2(1+K)[z_c m_c + z_s m_s]\right\}\frac{d\phi_0}{2\pi} \\ &= \frac{1+K}{\pi}\exp\left[-(1+K)(z_c^2+z_s^2) - K\right] \\ &\quad \cdot I_0\left[2\sqrt{K(1+K)(z_c^2+z_s^2)}\right] \end{aligned}$$

where the last step uses the identity $\int_{-\pi}^{\pi}\exp\left[a\cos(t+x) + b\sin(t+x)\right]dx = 2\pi I_0(\sqrt{a^2+b^2})$ [31, p.336].

Transforming the Cartesian coordinates (z_c, z_s) to polar coordinates (z, ψ) with $z_c = z\cdot\cos\psi$ and $z_s = z\cdot\sin\psi$, we obtain the transformation's Jacobian $J = z$; therefore, the joint PDF of the envelope $|Z|$ and the phase $\Psi = \arctan(z_c, z_s)$ is given by

$$\begin{aligned} f_{|Z|,\Psi}(z, \psi) &= \frac{(1+K)z}{\pi}\cdot\exp\left[-K-(1+K)z^2\right] \\ &\quad \cdot I_0\left[2z\sqrt{K(1+K)}\right], \quad z \geq 0,\ \psi \in [-\pi, \pi). \end{aligned}$$

Then, the marginal PDF's of the envelope and the phase can be obtained by the following two integrations

$$\begin{aligned} f_{|Z|}(z) &= \int_{-\pi}^{\pi} f_{|Z|,\Psi}(z, \psi)d\psi \\ &= 2(1+K)z\cdot\exp\left[-K-(1+K)z^2\right] \\ &\quad \cdot I_0\left[2z\sqrt{K(1+K)}\right], \quad z \geq 0 \\ f_{\Psi}(\psi) &= \int_0^{\infty} f_{|Z|,\Psi}(z, \psi)dz = \frac{1}{2\pi}, \quad \psi \in [-\pi, \pi) \end{aligned}$$

where the last equality utilizes the identity $\int_0^{\infty} x\exp(-ax^2)I_0(bx)dx = \frac{1}{2a}\exp\left(\frac{b^2}{4a}\right)$ [31, p.699]. This completes the proof. ■

We now highlight Theorem 6 with three remarks. First, both the fading envelope and the phase are stationary because their PDF's are independent of time t. This is very different from the previous Rician models [4], [16], where the PDF of the fading phase is a very complicated function of time t, and therefore the fading phase is not stationary as pointed out in [4]. Here, the fading phase of our new model is not only stationary but also uniformly distributed over $[-\pi, \pi)$. Second, the fading envelope and phase of our new Rician model are independent. As usual, the PDF's of the envelope and the phase of our Rician channel model include Rayleigh fading ($K = 0$) as a special case. Third, the PDF of the fading envelope of our Rician model can be derived by using the theory of two-dimensional random walks described in [35] and [36]. Details are omitted.

Two other important properties associated with the fading envelope are the *level-crossing rate* (LCR) and the *average fade duration* (AFD). Both of these represent higher-order behaviors that a high quality simulator should emulate accurately. The LCR is defined as the rate at which the envelope crosses a specified level with positive slope. The AFD is the average time duration that the fading envelope remains below a specified level after crossing below that level. Both the LCR and AFD provide important information for the statistics of burst errors [37], [38], which facilitates the design and selection of error correction techniques. Also, both represent practical behaviors of the simulator that depend on the higher-order statistics of the simulator. We now present explicit formulas for the LCR and AFD for a general Rician fading channel whose specular component has *non-zero* Doppler frequency. The following result (15a) is original while result (15b) represents a minor extension of a known result [30, p.66] for the case when the specular component is a constant.

Theorem 7: When N approaches infinity, the level-crossing rate $L_{|Z|}$ and the average fade duration $T_{|Z|}$ of the new

[1]The function $\arctan(x, y)$ maps the arguments (x, y) into a phase in the correct quadrant in $[-\pi, \pi)$.

simulator output are given by

$$L_{|Z|} = \sqrt{\frac{2(1+K)}{\pi}}\rho f_d \cdot \exp\left[-K-(1+K)\rho^2\right] \cdot \int_0^{\pi}\left[1+\frac{2}{\rho}\sqrt{\frac{K}{1+K}}\cos^2\theta_0\cdot\cos\alpha\right] \cdot \exp\left[2\rho\sqrt{K(1+K)}\cos\alpha - 2K\cos^2\theta_0\cdot\sin^2\alpha\right]d\alpha \tag{15a}$$

$$T_{|Z|} = \frac{1-Q\left[\sqrt{2K},\sqrt{2(1+K)\rho^2}\right]}{L_{|Z|}} \tag{15b}$$

where ρ is the normalized fading envelope level given by $|Z|/|Z|_{rms}$ with $|Z|_{rms}$ being the root-mean-square envelope level, and $Q(\cdot)$ is the first-order Marcum Q-function [39].

Proof: When N approaches infinity, the fading envelope is Rician distributed as shown in Theorem 6. Therefore, we can use the formula provided in [40] to obtain the LCR, $L_{|Z|}$, viz

$$L_{|Z|} = \int_0^{\infty} \dot{r} f(|Z|,\dot{r})d\dot{r},$$

where $\dot{r}$ is the envelope slope, $f(r,\dot{r})$ is the joint PDF of the envelope r and its slope $\dot{r}$ given by [40], [30]

$$f(r,\dot{r}) = \frac{r}{\sqrt{(2\pi)^3 B b_0}}\exp\left(-\frac{r^2+s^2}{2b_0}\right) \cdot \int_{-\pi}^{\pi}\exp\left[\frac{rs\cos\alpha}{b_0} - \frac{(b_0\dot{r}+b_1 s\sin\alpha)^2}{2Bb_0}\right]d\alpha$$

where, for our model defined in Definition 2, s, $B = b_0 b_2 - b_1^2$, b_0, b_1 and b_2 are given by

$$s = \sqrt{\frac{K}{1+K}}, \qquad b_0 = \frac{1}{2(1+K)}$$

$$b_1 = 2\pi b_0 \int_{-\pi}^{\pi}(f_d\cos\alpha - f_d\cos\theta_0)\frac{d\alpha}{2\pi} = -2\pi b_0 f_d\cos\theta_0$$

$$b_2 = (2\pi)^2 b_0 \int_{-\pi}^{\pi}(f_d\cos\alpha - f_d\cos\theta_0)^2\frac{d\alpha}{2\pi} = 2\pi^2 b_0 f_d^2\left(1+2\cos^2\theta_0\right)$$

$$B = 2\pi^2 b_0^2 f_d^2.$$

Using the procedure provided in [40] for deriving the LCR, we can validate (15a). Employing the procedure proposed in [30] for the AFD, we can obtain (15b). Details are omitted here for brevity. ∎

It is noted here that if $\theta_0 = \frac{\pi}{2}$ or $\theta_0 = -\frac{\pi}{2}$, which means that the specular component has *zero* Doppler frequency, then the LCR given by (15a) has a closed-form solution as follows

$$L_{|Z|} = \sqrt{2\pi(1+K)}\rho f_d \exp\left[-K-(1+K)\rho^2\right] \cdot I_0\left[2\rho\sqrt{K(1+K)}\right]. \tag{16}$$

This is the same solution as that given in [40] and [30] for the case of the specular component being deterministic. If $K=0$, $Z(t)=Y(t)$ becomes a Rayleigh fading process; then both the LCR and the AFD have closed-form solutions given by

$$L_{|Y|} = \sqrt{2\pi}\rho f_d e^{-\rho^2} \tag{17a}$$

$$T_{|Y|} = \frac{e^{\rho^2}-1}{\rho f_d\sqrt{2\pi}}. \tag{17b}$$

Before concluding this section, it is important to point out that the new simulation model can be directly used to generate multiple uncorrelated fading sample sequences for simulating frequency selective Rayleigh and/or Rician channels, MIMO channels, and diversity combining techniques. Let $Z_k(t)$ be the kth Rician (or Rayleigh with $K_k=0$) fading sample sequence given by

$$Z_k(t) = \sqrt{\frac{1}{1+K_k}}\sqrt{\frac{1}{N}}\sum_{n=1}^{N}\exp\left[jw_{d,k}t\cos\left(\frac{2\pi n+\theta_{n,k}}{N}\right)\right] \cdot \exp\left(j\phi_{n,k}\right) + \sqrt{\frac{K_k}{1+K_k}}\exp\left[j\left(w_{d,k}t\cos\theta_{0,k}+\phi_{0,k}\right)\right] \tag{18}$$

where $w_{d,k}$, K_k and $\theta_{0,k}$ are, respectively, the maximum radian Doppler frequency, the Rice factor and the specular component's angle of arrival of the kth Rician fading sample sequence, and where $\theta_{n,k}$, $\phi_{n,k}$ and $\phi_{0,k}$ are mutually independent and uniformly distributed over $[-\pi,\pi)$ for all n and k. Then, $Z_k(t)$ retains all the statistical properties of $Z(t)$ defined by eqn. (11). Furthermore, $Z_k(t)$ and $Z_l(t)$ are statistically independent for all $k \neq l$, due to the mutual independence of $\theta_{n,k}$, $\phi_{n,k}$, $\phi_{0,k}$, $\theta_{n,l}$, $\phi_{n,l}$ and $\phi_{0,l}$ when $k \neq l$.

IV. Empirical Testing

Verification of the proposed fading simulator is carried out by comparing the corresponding simulation results for finite N with those of the theoretical limit when N approaches infinity. Throughout the following discussions, the newly proposed statistical simulators have been implemented by choosing $N = 8$ unless otherwise specified. It is noted that if we choose a larger value for N, then the statistical accuracy of the simulator will be increased.

A. Correlation Statistics

We have conducted extensive simulations of the autocorrelations and cross-correlations of the quadrature components, and the autocorrelation of the complex envelope of both Rayleigh and Rician (with various Rice factors) fading signals. The simulation results of these correlation statistics match the theoretically calculated results with high accuracy even for small N. For example, Figs. 3 and 4 show the good agreement for the real part and imaginary part of the autocorrelation of the complex envelope of the fading. The simulation results and the theoretically calculated results for the autocorrelation of the squared envelope of the fading signals are slightly different when $N = 8$ as can be seen from Fig. 5. The differences decrease if we increase the value of N, as expected.

B. Envelope and Phase PDF's

Figs. 6 and 7 show that the PDF's of the fading envelope and phase of the simulator with $N = 8$ are in very good agreement with the theoretical ones. It is noted that when $N > 8$, these PDF's will have even better agreement with the theoretically desired ones. It is also noted that the more random samples used for the ensemble average in the simulations, the smaller the difference between the simulated curves and the desired reference curves for the phase PDF.

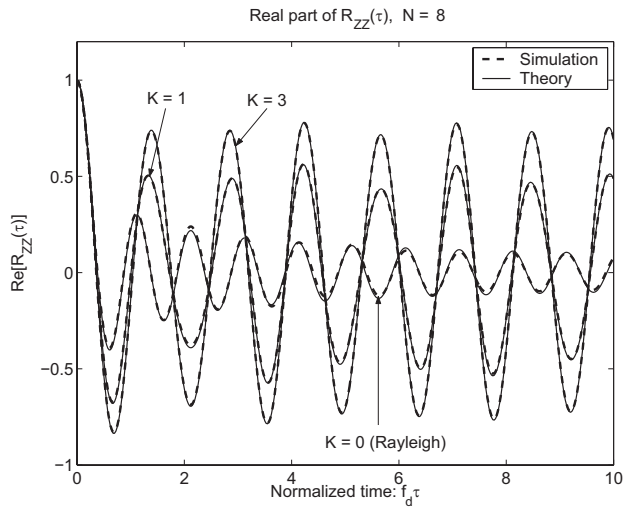

Fig. 3. The real part of the autocorrelation of the complex envelope $Z(t)$; $\theta_0 = \pi/4$ for $K = 1$ and $K = 3$ Rician cases.

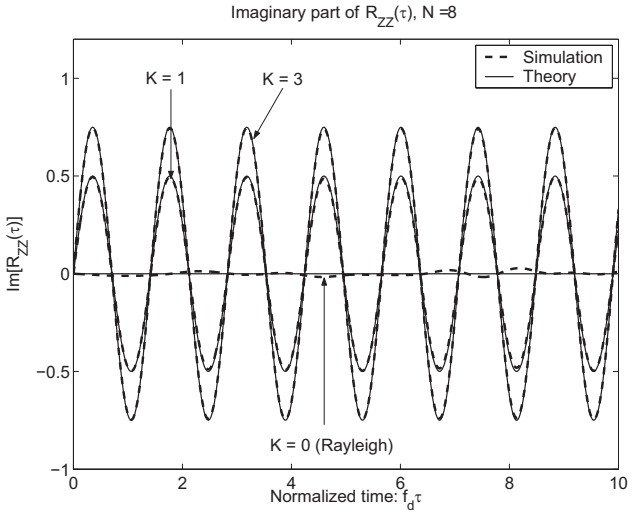

Fig. 4. The imaginary part of the autocorrelation of the complex envelope $Z(t)$; $\theta_0 = \pi/4$ for $K = 1$ and $K = 3$ Rician cases.

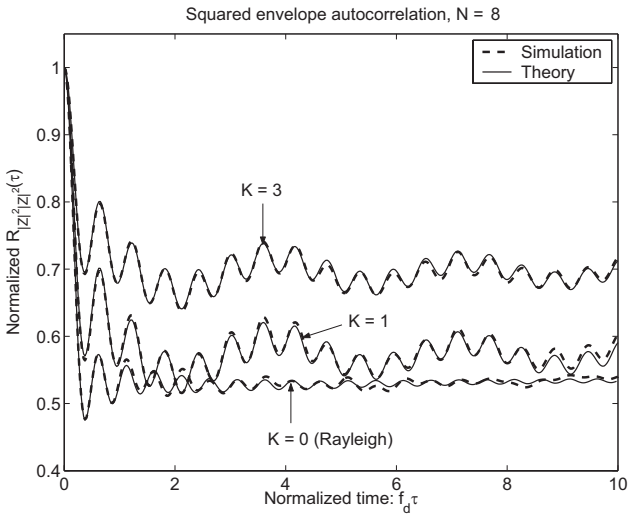

Fig. 5. The autocorrelation of the squared envelope $|Z(t)|^2$ with $\theta_0 = \pi/4$ for $K = 1$ and $K = 3$ Rician cases.

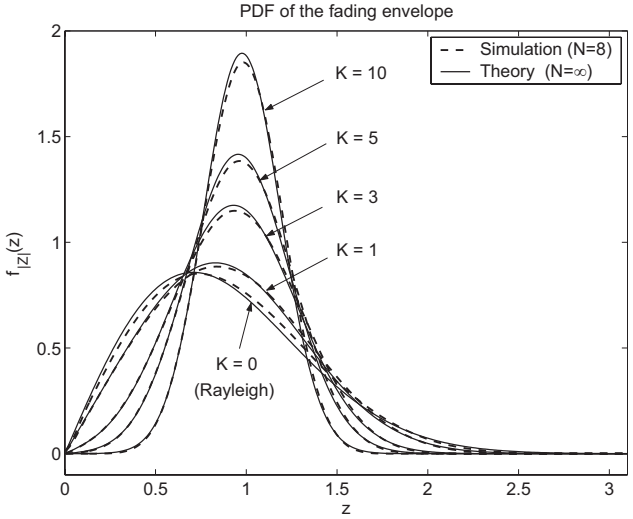

Fig. 6. The PDF of the fading envelope $|Z(t)|$.

C. LCR and AFD

The simulation results for the normalized level-crossing rate (LCR), $\frac{L_{|Z|}}{f_d}$, and the normalized average fade duration (AFD), $f_d T_{|Z|}$, of the new simulators are shown in Figs. 8 and 9, respectively, where the theoretically calculated LCR and AFD for $N = \infty$ are also included in the figures for comparison, indicating generally good agreement in both cases. Again, if we increase the number of sinusoids, N, the simulation results for the case of finite N approach the theoretical $N = \infty$ results.

For the region of $\rho < 0$ dB, it is interesting to note that the average fade duration for $\theta_0 = 0$ (or $\theta_0 < \pi/4$) tends to be smaller for larger values of the Rice factor K. This is different from the AFD for $\theta_0 = \pi/2$, which tends to be larger with larger Rice factors [30]. The main reason for this phenomenon is that when $\theta_0 = 0$, the Doppler frequency of the specular component is equal to the maximum Doppler frequency, f_d. For a given $\rho < 0$ dB and $K > 0$, the LCR is at its largest value and the AFD is at its smallest value. When the value of K is increased, the specular component becomes more dominant over the Rayleigh scatter components, and the AFD tends to be even smaller. However, when $\theta_0 = \pi/2$, the Doppler frequency of the specular component is zero, for each single trial and the AFD becomes larger when the value of K is increased.

V. Conclusion

In this paper, it was shown that Clarke's model with a finite number of sinusoids can be directly used for simulating Rayleigh fading channels, and its computational efficiency and second-order statistics are better than those of Jakes' original model [3] and as good as those of the recently improved Jakes' Rayleigh fading simulators [22], [24] and [25]. An improved Clarke's model was proposed to reduce the variance of the time averaged correlations of a fading realization from a single trial. A novel simulation model employing a random specular component was proposed for Rician fading channels. The specular (line-of-sight) component of this Rician fading model is a *zero-mean* stochastic sinusoid with a pre-chosen

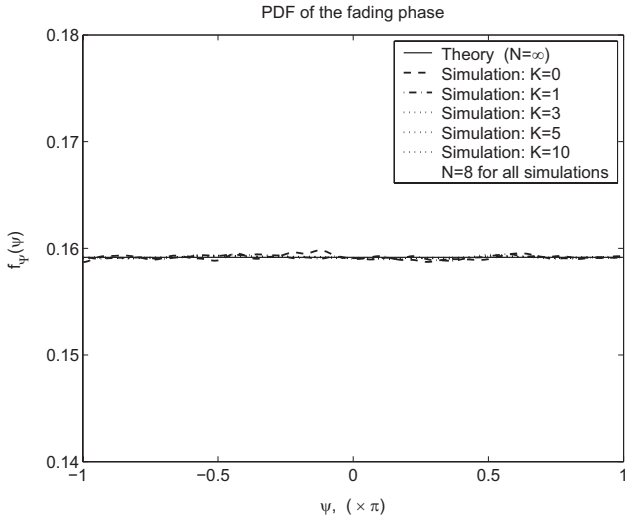

Fig. 7. The PDF of the fading phase $\Psi(t)$.

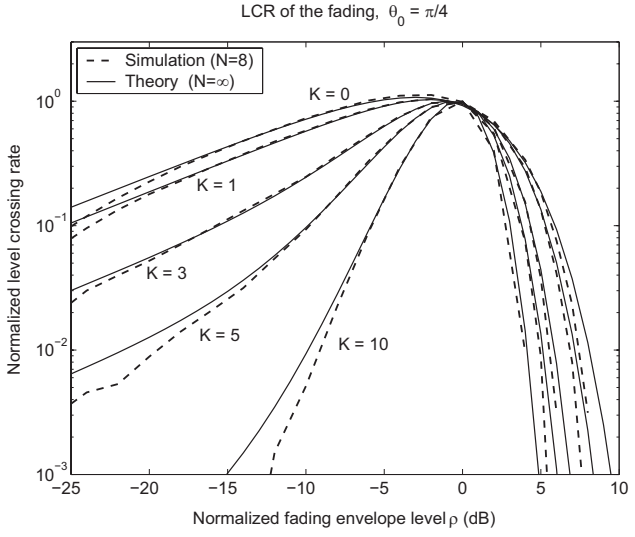

Fig. 8. The normalized LCR of the fading envelope $|Z(t)|$, where $\theta_0 = \pi/4$ for all $K > 0$ Rician fading.

Doppler frequency and a random initial phase. Compared to all the existing Rician fading simulation models, which have a *non-zero* deterministic specular component, the new model better reflects the fact that the specular component is random from ensemble sample to ensemble sample and from mobile to mobile. Additionally and importantly, the fading phase PDF of the new Rician fading model is independent of time and uniformly distributed over $[-\pi, \pi)$.

This paper has also analyzed the statistical properties of the new simulation models. Mathematical formulas were derived for the autocorrelation and cross-correlation of the quadrature components, the autocorrelation of the complex envelope and the squared envelope, the PDF's of the fading envelope and phase, the level-crossing rate and the average fade duration. It has been shown that all these statistics of the new simulators either exactly match or quickly converge to the desired ones. Good convergence can be reached even when the number of sinusoids is as small as 8.

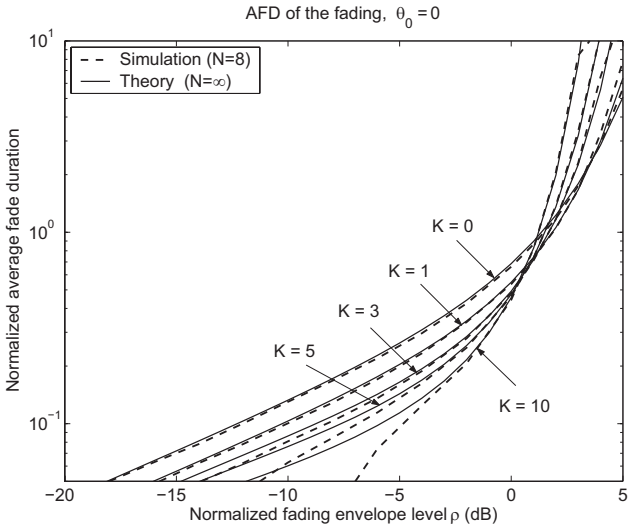

Fig. 9. The normalized AFD of the fading envelope $|Z(t)|$, where $\theta_0 = 0$ for all $K > 0$ Rician fading.

ACKNOWLEDGMENT

The first author, C. Xiao, is grateful to Drs. Q. Sun, H. Ye and W. Choi of Atheros Communications Inc. for pointing out an error in an earlier version of the manuscript. He is also indebted to Dr. F. Santucci and Professor G. L. Stuber for helpful discussions at the early stage of this work.

APPENDIX I
PROOF OF THEOREM 3

Proof: The autocorrelation function of the real part of the fading is proved first. One has

$$\begin{aligned}
R_{Y_cY_c}(\tau) &= E_{\alpha,\phi}\left[Y_c(t)Y_c(t+\tau)\right] \\
&= \frac{1}{N}\sum_{n=1}^{N}\sum_{i=1}^{N} E\left\{\cos(w_d t\cos\alpha_n + \phi_n)\right. \\
&\qquad \left.\cdot\cos[w_d(t+\tau)\cos\alpha_i + \phi_i]\right\} \\
&= \frac{1}{2N}\left\{\sum_{n=1}^{N} E[\cos(w_d\tau\cos\alpha_n)]\right\} \\
&= \frac{1}{2N}\left\{\sum_{n=1}^{N}\int_{-\pi}^{\pi}\cos\left[w_d\tau\cos\left(\frac{2\pi n+\theta_n}{N}\right)\right]\frac{d\theta_n}{2\pi}\right\} \\
&= \frac{1}{2N}\left\{\sum_{n=1}^{N}\int_{\frac{2\pi n-\pi}{N}}^{\frac{2\pi n+\pi}{N}}\cos\left(w_d\tau\cos\gamma_n\right)\frac{N}{2\pi}d\gamma_n\right\} \\
&= \frac{1}{4\pi}\int_{\frac{\pi}{N}}^{2\pi+\frac{\pi}{N}}\cos\left(w_d\tau\cos\gamma\right)d\gamma \\
&= \frac{1}{4\pi}\int_{0}^{2\pi}\cos(w_d\tau\cos\gamma)d\gamma \\
&= \frac{1}{2}J_0(w_d\tau).
\end{aligned}$$

Similarly, we can obtain the autocorrelation of the imagi-

nary part of the fading signal in (8a) as

$$\begin{aligned} R_{Y_sY_s}(\tau) &= E\left[Y_s(t)Y_s(t+\tau)\right] \\ &= \frac{1}{4\pi}\int_0^{2\pi}\cos(w_d\tau\cos\gamma)d\gamma \\ &= \frac{1}{2}J_0(w_d\tau). \end{aligned}$$

We are now in a position to prove equation (8b) starting from

$$\begin{aligned} R_{Y_cY_s}(\tau) &= E\left[Y_c(t)Y_s(t+\tau)\right] \\ &= \frac{1}{N}\sum_{n=1}^{N}\sum_{i=1}^{N}E\left\{\cos(w_dt\cos\alpha_n+\phi_n)\right. \\ &\qquad \left.\cdot\sin[w_d(t+\tau)\cos\alpha_i+\phi_i]\right\} \\ &= \frac{1}{2N}\sum_{n=1}^{N}E\left[\sin(w_d\tau\cos\alpha_n)\right] \\ &= \frac{1}{4\pi}\int_0^{2\pi}\sin(w_d\tau\cos\gamma)d\gamma = 0. \end{aligned}$$

The second part of eqns. (8b) and (8c) are proved in a similar manner. The proof of equation (8d) is different and lengthy. A brief outline with some salient details is given below. One has

$$\begin{aligned} R_{|Y|^2|Y|^2}(\tau) &= E\left[Y_c^2(t)Y_c^2(t+\tau)\right]+E\left[Y_s^2(t)Y_s^2(t+\tau)\right] \\ &\quad +E\left[Y_c^2(t)Y_s^2(t+\tau)\right]+E\left[Y_s^2(t)Y_c^2(t+\tau)\right]. \end{aligned} \tag{19}$$

The derivation of the first term on the right side of (19) in detail starts as

$$\begin{aligned} &E\left[Y_c^2(t)Y_c^2(t+\tau)\right] \\ &= \frac{1}{N^2}\cdot E\left\{\sum_{n=1}^{N}\cos(w_dt\cos\alpha_n+\phi_n)\right. \\ &\quad\cdot\sum_{i=1}^{N}\cos(w_dt\cos\alpha_i+\phi_i) \\ &\quad\cdot\sum_{p=1}^{N}\cos[w_d(t+\tau)\cos\alpha_p+\phi_p] \\ &\quad\left.\cdot\sum_{q=1}^{N}\cos[w_d(t+\tau)\cos\alpha_q+\phi_q]\right\}. \end{aligned} \tag{20}$$

Since the random phases ϕ_k and ϕ_l are statistically independent for all $k \neq l$, the right side of (20) is zero except for four different cases: a) $n=i=p=q$; b) $n=i$, $p=q$, and $n\neq p$; c) $n=p$, $i=q$, and $n\neq i$; and d) $n=q$, $i=p$, and $n\neq i$. Subsequently, $E\left[Y_c^2(t)Y_c^2(t+\tau)\right]$ is derived for each of the four cases.

For the first case, $n=i=p=q$, we have

$$\begin{aligned} &E\left[Y_c^2(t)Y_c^2(t+\tau)\right]_{1st} \\ &= \frac{1}{N^2}\sum_{n=1}^{N}E\left\{\cos^2(w_dt\cos\alpha_n+\phi_n)\right. \\ &\qquad\left.\cdot\cos^2[w_d(t+\tau)\cos\alpha_n+\phi_n]\right\} \\ &= \frac{1}{N^2}\left\{\sum_{n=1}^{N}E\left[\frac{1+\cos(2w_dt\cos\alpha_n+2\phi_n)}{2}\right.\right. \\ &\qquad\left.\left.\cdot\frac{1+\cos[2w_d(t+\tau)\cos\alpha_n+2\phi_n]}{2}\right]\right\} \\ &= \frac{1}{N^2}\left\{\frac{N}{4}+\frac{1}{8}\sum_{n=1}^{N}E[\cos(2w_d\tau\cos\alpha_n)]\right\} \\ &= \frac{1}{4N}+\frac{1}{8N}J_0(2w_d\tau). \end{aligned}$$

For the second case, $n=i$, $p=q$, and $n\neq p$, we have

$$\begin{aligned} &E\left[Y_c^2(t)Y_c^2(t+\tau)\right]_{2nd} \\ &= \frac{1}{N^2}\left\{\sum_{n=1}^{N}\sum_{\substack{p=1\\p\neq n}}^{N}E\left[\cos^2(w_dt\cos\alpha_n+\phi_n)\right]\right. \\ &\qquad\left.\cdot E\left(\cos^2[w_d(t+\tau)\cos\alpha_p+\phi_p]\right)\right\} \\ &= \frac{1}{N^2}\left[\frac{N^2-N}{4}\right] = \frac{1}{4}-\frac{1}{4N}. \end{aligned}$$

For the third case, $n=p$, $i=q$, and $n\neq i$, we have

$$\begin{aligned} &E\left[Y_c^2(t)Y_c^2(t+\tau)\right]_{3rd} \\ &= \frac{1}{N^2}\sum_{n=1}^{N}\sum_{\substack{i=1\\i\neq n}}^{N}E\left\{\cos(w_dt\cos\alpha_n+\phi_n)\right. \\ &\qquad\cdot\cos[w_d(t+\tau)\cos\alpha_n+\phi_n]\} \\ &\qquad\cdot E\left\{\cos(w_dt\cos\alpha_i+\phi_i)\right. \\ &\qquad\left.\cdot\cos[w_d(t+\tau)\cos\alpha_i+\phi_i]\right\} \\ &= \frac{1}{N^2}\left\{\sum_{n=1}^{N}\frac{1}{2}E[\cos(w_d\tau\cos\alpha_n)]\right\}^2 \\ &\quad-\frac{1}{N^2}\sum_{n=1}^{N}\left\{\frac{1}{2}E[\cos(w_d\tau\cos\alpha_n)]\right\}^2 \\ &= \frac{1}{4}J_0^2(w_d\tau)-\frac{f_c\left(w_d\tau,N\right)}{4}. \end{aligned}$$

For the fourth case, $n=q$, $i=p$, and $n\neq i$; in a manner similar to that used in the third case, one can prove

$$E\left[Y_c^2(t)Y_c^2(t+\tau)\right]_{4th} = \frac{1}{4}J_0^2(w_d\tau)-\frac{f_c\left(w_d\tau,N\right)}{4}.$$

Since these four cases are the exclusive and exhaustive possibilities for $E\left[Y_c^2(t)Y_c^2(t+\tau)\right]$ being non-zero, adding them together we have

$$\begin{aligned} &E\left[Y_c^2(t)Y_c^2(t+\tau)\right] \\ &= E\left[Y_c^2(t)Y_c^2(t+\tau)\right]_{1st}+E\left[Y_c^2(t)Y_c^2(t+\tau)\right]_{2nd} \\ &\quad+E\left[Y_c^2(t)Y_c^2(t+\tau)\right]_{3rd}+E\left[Y_c^2(t)Y_c^2(t+\tau)\right]_{4th} \\ &= \frac{1}{4}+\frac{1}{2}J_0^2(w_d\tau)+\frac{1}{8N}J_0(2w_d\tau)-\frac{f_c\left(w_d\tau,N\right)}{2}. \end{aligned}$$

This completes the derivation of $E\left[Y_c^2(t)Y_c^2(t+\tau)\right]$.

Using the same procedure for the second, third and fourth terms on the right side of (19), one obtains

$$\begin{aligned}
E\left[Y_s^2(t)Y_s^2(t+\tau)\right] &= \frac{1}{4}+\frac{1}{2}J_0^2(w_d\tau)+\frac{1}{8N}J_0(2w_d\tau) \\
&\quad -\frac{f_s\left(w_d\tau,N\right)}{2} \\
E\left[Y_c^2(t)Y_s^2(t+\tau)\right] &= \frac{1}{4}-\frac{1}{8N}J_0(2w_d\tau)-\frac{f_c\left(w_d\tau,N\right)}{2} \\
E\left[Y_s^2(t)Y_c^2(t+\tau)\right] &= \frac{1}{4}-\frac{1}{8N}J_0(2w_d\tau)-\frac{f_s\left(w_d\tau,N\right)}{2}.
\end{aligned}$$

Therefore,

$$R_{|Y|^2|Y|^2}(\tau)=1+J_0^2(w_d\tau)-f_c\left(w_d\tau,N\right)-f_s\left(w_d\tau,N\right).$$

This completes the proof of Theorem 3. ■

APPENDIX II
PROOF OF THEOREM 5

Proof: Based on the assumption that the initial phase of the specular component is uniformly distributed over $[-\pi,\pi)$, and independent of the initial phases of the scattered components, one can prove eqns. (12a)-(12c) by using the results of Theorem 3. The details are omitted for brevity. The proof of equation (12d) is outlined as follows. One has

$$\begin{aligned}
R_{|Z|^2|Z|^2}(\tau) &= E\left[Z_c^2(t)Z_c^2(t+\tau)\right]+E\left[Z_s^2(t)Z_s^2(t+\tau)\right] \\
&\quad +E\left[Z_c^2(t)Z_s^2(t+\tau)\right]+E\left[Z_s^2(t)Z_c^2(t+\tau)\right].
\end{aligned}$$

Then,

$$\begin{aligned}
&E\left[Z_c^2(t)Z_c^2(t+\tau)\right] \\
&= \frac{1}{(1+K)^2}E\left\{\left[Y_c(t)+\sqrt{K}\cos\left(w_dt\cos\theta_0+\phi_0\right)\right]^2\right. \\
&\quad \left.\cdot\left(Y_c(t+\tau)+\sqrt{K}\cos\left[w_d(t+\tau)\cos\theta_0+\phi_0\right]\right)^2\right\} \\
&= \frac{E\left[Y_c^2(t)Y_c^2(t+\tau)\right]}{(1+K)^2} \\
&\quad +\frac{K\cdot E\left[Y_c^2(t)\right]\cdot E\left\{\cos^2\left[w_d(t+\tau)\cos\theta_0+\phi_0\right]\right\}}{(1+K)^2} \\
&\quad +\frac{K\cdot E\left[Y_c^2(t+\tau)\right]\cdot E\left[\cos^2\left(w_dt\cos\theta_0+\phi_0\right)\right]}{(1+K)^2} \\
&\quad +\frac{4K\cdot E\left[Y_c(t)Y_c(t+\tau)\right]}{(1+K)^2}\cdot E\left\{\cos\left(w_dt\cos\theta_0+\phi_0\right)\right. \\
&\qquad \left.\cdot\cos\left[w_d(t+\tau)\cos\theta_0+\phi_0\right]\right\} \\
&\quad +\frac{K^2}{(1+K)^2}\cdot E\left\{\cos^2\left(w_dt\cos\theta_0+\phi_0\right)\right. \\
&\qquad \left.\cdot\cos^2\left[w_d(t+\tau)\cos\theta_0+\phi_0\right]\right\} \\
&= \frac{E\left[Y_c^2(t)Y_c^2(t+\tau)\right]}{(1+K)^2} \\
&\quad +\frac{K}{2(1+K)^2}\left[1+2J_0(w_d\tau)\cdot\cos(w_d\tau\cos\theta_0)\right] \\
&\quad +\frac{K^2}{4(1+K)^2}\left[1+\frac{\cos(2w_d\tau\cos\theta_0)}{2}\right].
\end{aligned}$$

Similarly, we have

$$\begin{aligned}
&E\left[Z_s^2(t)Z_s^2(t+\tau)\right] \\
&= \frac{1}{(1+K)^2}E\left\{\left[Y_s(t)+\sqrt{K}\sin\left(w_dt\cos\theta_0+\phi_0\right)\right]^2\right. \\
&\quad \left.\cdot\left(Y_s(t+\tau)+\sqrt{K}\sin\left[w_d(t+\tau)\cos\theta_0+\phi_0\right]\right)^2\right\} \\
&= \frac{E\left[Y_s^2(t)Y_s^2(t+\tau)\right]}{(1+K)^2} \\
&\quad +\frac{K}{2(1+K)^2}\left[1+2J_0(w_d\tau)\cdot\cos(w_d\tau\cos\theta_0)\right] \\
&\quad +\frac{K^2}{4(1+K)^2}\left[1+\frac{\cos(2w_d\tau\cos\theta_0)}{2}\right]
\end{aligned}$$

and

$$\begin{aligned}
&E\left[Z_c^2(t)Z_s^2(t+\tau)\right] \\
&= \frac{1}{(1+K)^2}E\left\{\left[Y_c(t)+\sqrt{K}\cos\left(w_dt\cos\theta_0+\phi_0\right)\right]^2\right. \\
&\quad \left.\cdot\left(Y_s(t+\tau)+\sqrt{K}\sin\left[w_d(t+\tau)\cos\theta_0+\phi_0\right]\right)^2\right\} \\
&= \frac{E\left[Y_c^2(t)Y_s^2(t+\tau)\right]}{(1+K)^2} \\
&\quad +\frac{K\cdot E\left[Y_c^2(t)\right]\cdot E\left\{\sin^2\left[w_d(t+\tau)\cos\theta_0+\phi_0\right]\right\}}{(1+K)^2} \\
&\quad +\frac{K\cdot E\left[Y_s^2(t+\tau)\right]\cdot E\left[\cos^2\left(w_dt\cos\theta_0+\phi_0\right)\right]}{(1+K)^2} \\
&\quad +\frac{K^2}{(1+K)^2}\cdot E\left\{\cos^2\left(w_dt\cos\theta_0+\phi_0\right)\right. \\
&\qquad \left.\cdot\sin^2\left[w_d(t+\tau)\cos\theta_0+\phi_0\right]\right\} \\
&= \frac{E\left[Y_c^2(t)Y_s^2(t+\tau)\right]}{(1+K)^2}+\frac{K}{2(1+K)^2} \\
&\quad +\frac{K^2}{4(1+K)^2}\left[1-\frac{\cos(2w_d\tau\cos\theta_0)}{2}\right]
\end{aligned}$$

and

$$\begin{aligned}
&E\left[Z_s^2(t)Z_c^2(t+\tau)\right] \\
&= \frac{1}{(1+K)^2}E\left\{\left[Y_s(t)+\sqrt{K}\sin\left(w_dt\cos\theta_0+\phi_0\right)\right]^2\right. \\
&\quad \left.\cdot\left(Y_c(t+\tau)+\sqrt{K}\cos\left[w_d(t+\tau)\cos\theta_0+\phi_0\right]\right)^2\right\} \\
&= \frac{E\left[Y_c^2(t)Y_s^2(t+\tau)\right]}{(1+K)^2}+\frac{K}{2(1+K)^2} \\
&\quad +\frac{K^2}{4(1+K)^2}\left[1-\frac{\cos(2w_d\tau\cos\theta_0)}{2}\right].
\end{aligned}$$

Therefore,

$$\begin{aligned}
&R_{|Z|^2|Z|^2}(\tau) \\
&= \frac{R_{|Y|^2|Y|^2}(\tau)+K^2+2K\left[1+J_0(w_d\tau)\cos(w_d\tau\cos\theta_0)\right]}{(1+K)^2} \\
&= \frac{1+J_0^2(w_d\tau)+K^2+2K\left[1+J_0(w_d\tau)\cos(w_d\tau\cos\theta_0)\right]}{(1+K)^2} \\
&\quad -\frac{f_c(w_d\tau,N)+f_s(w_d\tau,N)}{(1+K)^2}
\end{aligned}$$

This completes the proof. ■

REFERENCES

[1] R. H. Clarke, "A statistical theory of mobile-radio reception," *Bell Syst. Tech. J.*, pp. 957-1000, Jul.-Aug. 1968.

[2] M. J. Gans, "A power-spectral theory of propagation in the mobile-radio environment," *IEEE Trans. Veh. Technol.*, vol. 21, pp. 27-38, Feb. 1972.

[3] W. C. Jakes, *Microwave Mobile Communications*. Wiley, 1974; re-issued by IEEE Press, 1994.

[4] T. Aulin, "A modified model for the fading signal at a mobile radio channel," *IEEE Trans. Veh. Technol.*, vol. 28, pp. 182-203, Aug. 1979.

[5] A. A. M. Saleh and R. A. Valenzuela, "A statistical model for indoor multipath propagation," *IEEE J. Select. Areas Commun.*, vol. 5, pp. 128-137, Feb. 1987.

[6] W. R. Braun and U. Dersch, "A physical mobile radio channel model," *IEEE Trans. Veh. Technol.*, vol. 40, pp. 472-482, May 1991.

[7] P. Hoeher, "A statistical discrete-time model for the WSSUS multipath channel," *IEEE Trans. Veh. Technol.*, vol. 41, pp. 461-468, Nov. 1992.

[8] S. A. Fechtel, "A novel approach to modeling and efficient simulation of frequency-selective fading radio channels," *IEEE J. Select. Areas Commun.*, vol. 11, pp. 422-431, Apr. 1993.

[9] P. Dent, G. E. Bottomley, and T. Croft, "Jakes fading model revisited," *IEEE Electron. Lett.*, vol. 29, pp. 1162-1163, June 1993.

[10] H. Hashemi, "The indoor radio propagation channel," *Proc. IEEE*, vol. 81, pp. 943-968, July 1993.

[11] U. Dersch and R. J. Ruegg, "Simulations of the time and frequency selective outdoor mobile radio channel," *IEEE Trans. Veh. Technol.*, vol. 42, pp. 338-344, Aug. 1993.

[12] P. M. Crespo and J. Jimenez, "Computer simulation of radio channels using a harmonic decomposition technique," *IEEE Trans. Veh. Technol.*, vol. 44, pp. 414-419, Aug. 1995.

[13] K.-W. Yip and T.-S. Ng, "Discrete-time model for digital communications over a frequency-selective Rician fading WSSUS channel," *IEE Proc. Commun.*, vol. 143, pp. 37-42, Feb. 1996.

[14] K.-W. Yip and T.-S. Ng, "Karhunen-Loeve expansion of the WSSUS channel output and its application to efficient simulation," *IEEE J. Select. Areas Commun.*, vol. 15, pp. 640-646, May 1997.

[15] A. Anastasopoulos and K. M. Chugg, "An efficient method for simulation of frequency selective isotropic Rayleigh fading," in *Proc. IEEE VTC*, vol. 3, pp. 2084-2088, May 1997.

[16] M. Patzold, U. Killat, F. Laue, and Y. Li, "On the statistical properties of deterministic simulation models for mobile fading channels," *IEEE Trans. Veh. Technol.*, vol. 47, pp. 254-269, Feb. 1998.

[17] Y. X. Li and X. Huang, "The generation of independent Rayleigh faders," in *Proc. IEEE ICC*, June 2000, vol. 1, pp. 41-45; also *IEEE Trans. Commun.*, vol. 50, pp. 1503-1514, Sep. 2002.

[18] K.-W. Yip and T.-S. Ng, "A simulation model for Nakagami-m fading channels, $m < 1$," *IEEE Trans. Commun.*, vol. 48, pp. 214-221, Feb. 2000.

[19] M. F. Pop and N. C. Beaulieu, "Limitations of sum-of-sinusoids fading channel simulators," *IEEE Trans. Commun.*, vol. 49, pp. 699-708, Apr. 2001.

[20] E. Chiavaccini and G. M. Vitetta, "GQR models for multipath Rayleigh fading channels," *IEEE J. Select. Areas Commun.*, vol. 19, pp. 1009-1018, June 2001.

[21] M. F. Pop and N. C. Beaulieu, "Design of wide-sense stationary sum-of-sinusoids fading channel simulators," in *Proc. IEEE ICC*, Apr. 2002, pp. 709-716.

[22] C. Xiao and Y. R. Zheng, "A generalized simulation model for Rayleigh fading channels with accurate second-order statistics," in *Proc. IEEE VTC-Spring*, May 2002, pp. 170-174.

[23] C. Xiao, Y. R. Zheng, and N. C. Beaulieu, "Second-order statistical properties of the WSS Jakes' fading channel simulator," *IEEE Trans. Commun.*, vol. 50, pp. 888-891, June 2002.

[24] Y. R. Zheng and C. Xiao, "Improved models for the generation of multiple uncorrelated Rayleigh fading waveforms," *IEEE Commun. Lett.*, vol. 6, pp. 256-258, June 2002.

[25] Y. R. Zheng and C. Xiao, "Simulation models with correct statistical properties for Rayleigh fading channels," *IEEE Trans. Commun.*, vol. 51, pp. 920-928, June 2003.

[26] F. Vatta, G. Montorsi, and F. Babich, "Achievable performance of turbo codes over the correlated Rician channel," *IEEE Trans. Commun.*, vol. 51, pp. 1-4, Jan. 2003.

[27] S. Gazor and H. S. Rad, "Space-time coding ambiguities in joint adaptive channel estimation and detection," *IEEE Trans. Signal Processing*, vol. 52, pp. 372-384, Feb. 2004.

[28] F. Babich, "On the performance of efficient coding techniques over fading channels," *IEEE Trans. Wireless Commun.*, vol. 3, pp. 290-299, Jan. 2004.

[29] J. Liu, Y. Yuan, L. Xu, R. Wu, Y. Dai, Y. Li, L. Zhang, M. Shi, and Y. Du, "Research on smart antenna technology for terminals for the TD-SCDMA system," *IEEE Commun. Mag.*, vol. 41, pp. 116-119, June 2003.

[30] G. L. Stuber, *Principles of Mobile Communication*, 2nd ed. Norwell, MA: Kluwer Academic Publishers, 2001.

[31] I. S. Gradshteyn and I. M. Ryzhik, *Table of Integrals, Series, and Products*, 6th ed. A. Jeffrey, ed. (San Diego: Academic Press, 2000).

[32] Qinfang Sun, Huanchun Ye, and Won-Joon Choi, Private Communications, Feb. 9, 2004.

[33] C. S. Patel, G. L. Stuber, and T. G. Pratt, "Comparative analysis of statistical models for the simulation of Rayleigh faded cellular channels," *IEEE Trans. Commun.*, vol. 53, pp. 1017-1026, June 2005.

[34] J. G. Proakis, *Digital Communications*, 4th ed. New York: McGraw Hill, 2001.

[35] M. Slack, "The probability distributions of sinusoidal oscillations combined in random phase," *IEE Proceedings*, vol. 93, pp. 76-86, 1946.

[36] W. R. Bennett, "Distribution of the sum of randomly phased components," *Quart. Appl. Math.*, vol. 5, pp. 385-393, Jan. 1948.

[37] K. Ohtani, K. Daikoku, and H. Omori, "Burst error performance encountered in digital land mobile radio channel," *IEEE Trans. Veh. Technol.*, vol. 30, no. 4, pp. 156-160, Nov. 1981.

[38] J. M. Morris, "Burst error statistics of simulated Viterbi decoded BPSK on fading and scintillating channels," *IEEE Trans. Commun.*, vol. 40, pp. 34-41, 1992.

[39] M. K. Simon and M.-S. Alouini, *Digital Communication over Fading Channels*, 2nd ed. New York: John Wiley & Sons, 2005.

[40] S. O. Rice, "Statistical properties of a sine wave plus random noise," *Bell Syst. Tech. J.*, vol. 27, pp. 109-157, Jan. 1948.

Chengshan Xiao (M'99-SM'02) received the B.S. degree from the University of Electronic Science and Technology of China, Chengdu, China, in 1987, the M.S. degree from Tsinghua University, Beijing, China, in 1989, and the Ph.D. degree from the University of Sydney, Sydney, Australia, in 1997, all in electrical engineering.

From 1989 to 1993, he was on the Research Staff and then became a Lecturer with the Department of Electronic Engineering at Tsinghua University, Beijing, China. From 1997 to 1999, he was a Senior Member of Scientific Staff at Nortel Networks, Ottawa, ON, Canada. From 1999 to 2000, he was an faculty member with the Department of Electrical and Computer Engineering at the University of Alberta, Edmonton, AB, Canada. Since 2000, he has been with the Department of Electrical and Computer Engineering at the University of Missouri-Columbia, where he is currently an Associate Professor. His research interests include wireless communication networks, signal processing, and multidimensional and multirate systems. He has published extensively in these areas. He holds three U.S. patents in wireless communications area. His algorithms have been implemented into Nortel's base station radios with successful technical field trials and network integration.

Dr. Xiao is a member of the IEEE Technical Committee on Personal Communications (TCPC) and the IEEE Technical Committee on Communication Theory. He served as a Technical Program Committee member for a number of IEEE international conferences including WCNC, ICC and Globecom in the last few years. He was a Vice Chair of the 2005 IEEE Globecom Wireless Communications Symposium. He is currently the Vice Chair of the TCPC of the IEEE Communications Society. He has been an Editor for the *IEEE Transactions on Wireless Communications* since July 2002. Previously, he was an Associate Editor for the *IEEE Transactions on Vehicular Technology* from July 2002 to June 2005, the *IEEE Transactions on Circuits and Systems-I* from January 2002 to December 2003, and the international journal of *Multidimensional Systems and Signal Processing* from January 1998 to December 2005.

Yahong Rosa Zheng (S'99-M'03) received the B.S. degree from the University of Electronic Science and Technology of China, Chengdu, China, in 1987, the M.S. degree from Tsinghua University, Beijing, China, in 1989, both in electrical engineering. She received the Ph.D. degree from the Department of Systems and Computer Engineering, Carleton University, Ottawa, ON, Canada, in 2002.

From 1989 to 1997, she held Engineer positions in several companies. From 2003 to 2005, she was a Natural Science and Engineering Research Council of Canada (NSERC) Postdoctoral Fellow at the University of Missouri, Columbia, MO. Currently, she is an Assistant Professor with the Department of Electrical and Computer Engineering at the University of Missouri, Rolla, MO. Her research interests include array signal processing, wireless communications, and wireless sensor networks.

Dr. Zheng has served as a Technical Program Committee member for the 2004 IEEE International Sensors Conference, the 2005 IEEE Global Telecommunications Conference, and the 2006 IEEE International Conference on Communications. Dr. Zheng is currently an Editor for the *IEEE Transactions on Wireless Communications*.

Norman C. Beaulieu (S'82-M'86-SM'89-F'99) received the B.A.Sc. (honors), M.A.Sc., and Ph.D degrees in electrical engineering from the University of British Columbia, Vancouver, BC, Canada in 1980, 1983, and 1986, respectively. He was awarded the University of British Columbia Special University Prize in Applied Science in 1980 as the highest standing graduate in the faculty of Applied Science.

He was a Queen's National Scholar Assistant Professor with the Department of Electrical Engineering, Queen's University, Kingston, ON, Canada from September 1986 to June 1988, an Associate Professor from July 1988 to June 1993, and a Professor from July 1993 to August 2000. In September 2000, he became the *i*CORE Research Chair in Broadband Wireless Communications at the University of Alberta, Edmonton, AB, Canada and in January 2001, the Canada Research Chair in Broadband Wireless Communications. His current research interests include broadband digital communications systems, ultra-wide bandwidth systems, fading channel modeling and simulation, diversity systems, interference prediction and cancellation, importance sampling and semi-analytical methods, and space-time coding.

Dr. Beaulieu is a Member of the IEEE Communication Theory Committee and served as its Representative to the Technical Program Committee of the 1991 International Conference on Communications and as Co-Representative to the Technical Program Committee of the 1993 International Conference on Communications and the 1996 International Conference on Communications. He was General Chair of the Sixth Communication Theory Mini-Conference in association with GLOBECOM 97 and Co-Chair of the Canadian Workshop on Information Theory 1999. He has been an Editor for Wireless Communication Theory of the *IEEE Transactions on Communications* since January 1992, and was Editor-in-Chief from January 2000 to December 2003. He served as an Associate Editor for Wireless Communication Theory of the *IEEE Communications Letters* from November 1996 to August 2003. He has also served on the Editorial Board of the *Proceedings of the IEEE* since November 2000. He received the Natural Science and Engineering Research Council of Canada (NSERC) E.W.R. Steacie Memorial Fellowship in 1999. Professor Beaulieu was elected a Fellow of the Engineering Institute of Canada in 2001 and was awarded the Medaille K.Y. Lo Medal of the Institute in 2004. He was elected Fellow of the Royal Society of Canada in 2002 and was awarded the Thomas W. Eadie Medal of the Society in 2005.